AGU PUBLICATIONS

Geophysical Research Letters

RESEARCH LETTER
10.1002/2014GL061747

Key Points:
- Titan's plasma environment responds to global changes in hot plasma pressure
- Titan is exposed to highly variable upstream plasma beta and dynamic pressure
- Including hot plasma variability improves agreement between models and data

Supporting Information:
- Readme
- Figure S1
- Figure S2
- Figure S3
- Text S1

Correspondence to:
N. Achilleos,
nicholas.achilleos@ucl.ac.uk

Citation:
Achilleos, N., C. S. Arridge, C. Bertucci, P. Guio, N. Romanelli, and N. Sergis (2014), A combined model of pressure variations in Titan's plasma environment, *Geophys. Res. Lett.*, *41*, 8730–8735, doi:10.1002/2014GL061747.

Received 12 SEP 2014
Accepted 11 NOV 2014
Accepted article online 17 NOV 2014
Published online 29 DEC 2014

A combined model of pressure variations in Titan's plasma environment

N. Achilleos[1,2,3], C. S. Arridge[2,4,5], C. Bertucci[6], P. Guio[1,2], N. Romanelli[6], and N. Sergis[7]

[1]Department of Physics and Astronomy, University College London, London, UK, [2]Centre for Planetary Sciences at UCL/Birkbeck, University College London, London, UK, [3]Japan Aerospace Exploration Agency Institute of Space and Astronautical Science, Sagamihara, Japan, [4]Mullard Space Science Laboratory, Dorking, UK, [5]Department of Physics, Lancaster University, Lancaster, UK, [6]Instituto de Astronomía y Física del Espacio, University of Buenos Aires, Buenos Aires, Argentina, [7]Office for Space Research and Technology, Academy of Athens, Athens, Greece

Abstract In order to analyze varying plasma conditions upstream of Titan, we have combined a physical model of Saturn's plasma disk with a geometrical model of the oscillating current sheet. During modeled oscillation phases where Titan is farthest from the current sheet, the main sources of plasma pressure in the near-Titan space are the magnetic pressure and, for disturbed conditions, the hot plasma pressure. When Titan is at the center of the sheet, the main sources are the dynamic pressure associated with Saturn's cold, subcorotating plasma and the hot plasma pressure under disturbed conditions. Total pressure at Titan (dynamic plus thermal plus magnetic) typically increases by a factor of up to about 3 as the current sheet center is approached. The predicted incident plasma flow direction deviates from the orbital plane of Titan by $\lesssim 10°$. These results suggest a correlation between the location of magnetic pressure maxima and the oscillation phase of the plasma sheet. Our model may be used to predict near-Titan conditions from "far-field" in situ measurements.

1. Introduction

Titan is usually embedded within the rotating magnetosphere of Saturn, a configuration which leads to the formation of a "flow-induced" magnetosphere, via the draping of the magnetic field in the subcorotating flow about the moon (Titan's orbital speed of ~6 km s^{-1} is small compared to the typical speed of the rotating plasma, ~120 km s^{-1}). Recently, *Bertucci et al.* [2009] demonstrated, using Cassini data, that the direction and magnitude of the magnetic field upstream of Titan vary, depending mainly on whether Titan is located above or below Saturn's magnetospheric current sheet. Titan's distance from the current sheet is influenced by global magnetospheric oscillations at Saturn, which change the elevation of the current sheet with respect to the rotational equatorial plane. The sheet geometry was modeled by *Arridge et al.* [2011b] (hereafter A11).

In Figure 1, we plot one example of current sheet elevation, Z_{CS}, from this A11 model. For constant radial distance (e.g., along Titan's orbit), Z_{CS} will vary with azimuth, i.e., there is a "ripple" in the sheet surface. For southern summer, Z_{CS} is everywhere positive; hence, the azimuthally averaged surface forms a "bowl-like" shape. We have combined the A11 model of sheet geometry with the Saturn plasma disk model of *Achilleos et al.* [2010a] (hereafter Ach10), updated by *Achilleos et al.* [2010b], in order to predict the variable magnetic and plasma parameters during the T15 encounter of Titan by the Cassini spacecraft (closest approach occurred on 2 July 2006 at 09:21 UTC, at altitude ~1900 km). This analysis enables us to predict the variations which arise from plasma sheet oscillations. In future, we aim to repeat the analysis for additional Titan encounters, and so provide a theoretical analog of observational classifications of the Titan environment, such as those of *Rymer et al.* [2009] and *Simon et al.* [2010]. We have also chosen T15 for the present analysis because we have obtained relevant plasma moment data which we compare with our model results herein.

In section 2, we describe a combined model which employs the A11 current sheet geometry with the Ach10 magnetic field/plasma model. The "Ach10" model we use is an updated version of the original model by *Achilleos et al.* [2010a], modified to include more realistic plasma parameters based on observations [*Achilleos et al.*, 2010b]. In section 3, we implement this model and compare it to observations of the magnetic field, magnetic pressure, and hot plasma pressure for several magnetospheric oscillation periods centered on the T15 Titan flyby (hot plasma pressure refers to H+ and O+ ions with energies >3 keV [*Sergis et al.*, 2009]). We summarize and give conclusions in section 4.

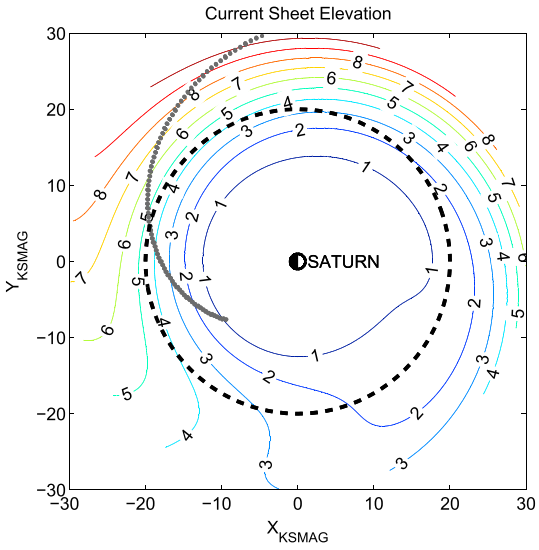

Figure 1. Plasma sheet geometry: Contours indicate the altitude Z_{CS} (in units of Saturn radii R_S) of the A11 model current sheet above Saturn's rotational equator (see text). The geometry shown is for southern summer. The black, dashed circle is Titan's orbit, and the gray squares represent a curve of constant "phase" in the sheet—this curve passes through the point of maximum Z_{CS} at each radial distance. The X_{KSMAG} axis is the intersection of the rotational equator and the noon meridian of Saturn local time (SLT). The whole pattern rotates with a variable period, following that of the SKR.

2. Plasma Disk Model Description

For this study, we require a "two-component" model of Saturn's plasma disk. The first component is the A11 geometrical model of the current sheet, illustrated in Figure 1. For cylindrical radial distance exceeding ~12 R_S, the altitude Z_{CS} of the current sheet (with respect to Saturn's rotational equator) is given by A11:

$$Z_{CS} = [\rho - R_H \tanh(\rho/R_H)] \tan(-\theta_\odot) + \tan(\theta_T)(\rho - \rho_o)\cos(\lambda), \quad \rho > 12\,R_S \quad (1)$$

where the first term represents the axisymmetric bowl and the second term the spatial oscillation, or ripple. Symbols have the following meanings: ρ is cylindrical radial distance with respect to the planet's rotational/magnetic axis, R_H is the hinging distance which controls the curvature of the bowl, $\theta_\odot$ is the subsolar latitude at Saturn (positive for northern latitude, negative for southern), θ_T is an effective angle of tilt for the current sheet, $\rho_o = 12\,R_S$ is a scaling distance which controls the amplitude of the ripple. λ represents the following phase angle for describing plasma sheet oscillation, dependent on both position and time:

$$\lambda = \lambda_{SLS3} - \lambda_o - \Omega_{SKR}(\rho - \rho_o)/V_{WAVE}, \quad (2)$$

where SLS3 denotes the longitude of *Kurth et al.* [2008], based on fitting a low-order polynomial to the nonstationary period of the Saturn Kilometric Radiation (SKR). Since SLS3 was developed, distinct SKR signals have been identified in Saturn's northern and southern hemisphere [e.g., *Lamy*, 2011]—the SLS3 phase lies consistently within ~30° of that of the southern SKR source [*Andrews et al.*, 2010]. A "prime meridian" parameter denoted by λ_o is fitted by A11 to different passes of Cassini data. Ω_{SKR} is a variable angular velocity corresponding to the SLS3 period. V_{WAVE} is a "wave speed" parameter which introduces a systematic delay of the oscillation phase with radial distance (see Figure 1). The T15 Titan encounter occurred during Cassini's Revolution 25. We thus adopt sheet parameters consistent with those used by A11 for their Rev 25 model fit, namely, $\lambda_o = 100°$, $V_{WAVE} = 5\,R_S\,h^{-1}$, $R_H = 16\,R_S$, $\theta_T = 12°$, $\rho_o = 12\,R_S$.

The second component of our plasma disk model provides magnetic field and plasma distributions for an axisymmetric, rotating magnetosphere in force balance (see Ach10 and supporting information). The Ach10 model assumes north-south symmetry, with a current sheet lying in the rotational equator. Any plasma parameter is a function of two coordinates, e.g., ρ_μ and Z_μ, the respective cylindrical radial distance and altitude (with respect to the rotational equator) in the "Ach10 model space." In order to combine the Ach10 model with the A11 sheet geometry, we calculate "equivalent Ach10 model coordinates" corresponding to the spacecraft's actual location:

$$\rho_\mu = \rho_{S/C}, Z_\mu = (Z_{S/C} - Z_{CS})\,\hat{\boldsymbol{z}} \cdot \hat{\boldsymbol{n}}, r_\mu = (\rho_\mu^2 + Z_\mu^2)^{1/2}, \cos\theta_\mu = Z_\mu / r_\mu, \quad (3)$$

where $\rho_{S/C}$ is the spacecraft's actual cylindrical radial distance from the planet's rotation / dipole axis, $Z_{S/C}$ and Z_{CS} are the respective altitudes of the spacecraft and the A11 current sheet with respect to the rotational equator, $\hat{\boldsymbol{z}}$ is a unit vector pointing in the northern direction of the planet's axis, and $\hat{\boldsymbol{n}}$ is the unit vector normal to the A11 current sheet at the distance $\rho = \rho_{S/C}$. These expressions assume that the local structure of the disk plasma (at Cassini) may be approximated by a version of the Ach10 model, whose plane of symmetry has been rotated to match the local tangent plane of the A11 sheet.

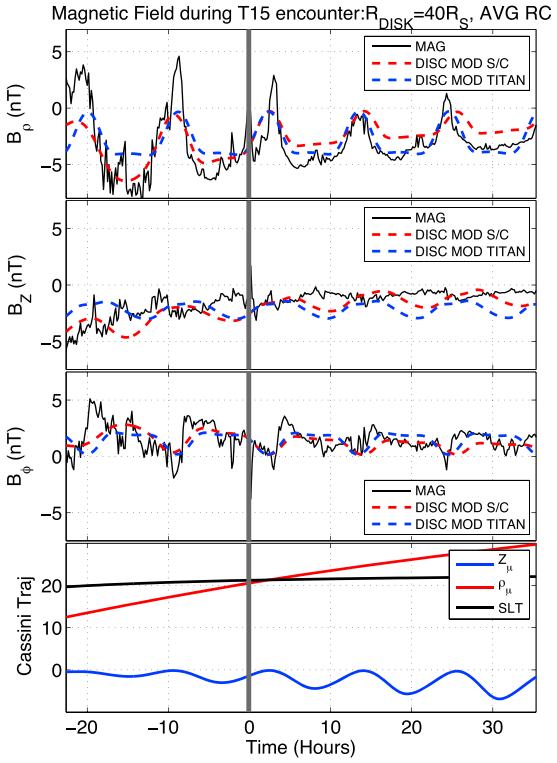

Figure 2. (first to third panels) Cylindrical components of the magnetic field (in units of nano-Tesla, nT) observed by Cassini, and predicted by the model, during several magnetospheric oscillations before and after the T15 wake crossing (vertical gray line). The zero of time indicates closest approach to Titan. Plotted data were generated by smoothing the magnetometer (MAG) 1 min averaged data (cadence of 1 min) using a 10-point boxcar filter, then downsampling to one sample every 10 min. Model fields for both Cassini and Titan-center-based observers are shown. (fourth panel) Equivalent Ach10 model coordinates along the spacecraft trajectory. Z_μ indicates perpendicular distance from the spacecraft to the A11 current sheet.

The final form of the model field components is given by an internal centered dipole (Ach10), aligned with Saturn's rotation axis, combined with an external component "anchored" to the A11 geometry, as follows:

$$\boldsymbol{B} = \boldsymbol{B}_{\mathbf{dip}} + \boldsymbol{B}_{\mathbf{ext}},\ \ \boldsymbol{B}_{\mathbf{ext}} = \Delta B_\rho\,\hat{\rho}_{CS} + \Delta B_Z\,\hat{\boldsymbol{n}} + B_\phi\,\hat{\boldsymbol{\phi}}_{CS},\ \ \hat{\rho}_{CS} = \frac{\hat{\boldsymbol{\phi}}_{ROT}\times\hat{\boldsymbol{n}}}{|\hat{\boldsymbol{\phi}}_{ROT}\times\hat{\boldsymbol{n}}|}, \hat{\boldsymbol{\phi}}_{CS} = \hat{\boldsymbol{n}}\times\hat{\rho}_{CS} \tag{4}$$

where the ΔB quantities are the cylindrical external field components (total field minus internal dipole) from the Ach10 model, interpolated on the model grid at "equivalent coordinates" $r_\mu, \cos\theta_\mu$ from equation (3). The ΔB represents external currents and include a minor magnetopause "shielding field." Unit vectors $\hat{\rho}_{CS}$, $\hat{\boldsymbol{\phi}}_{CS}$ lie in the tangent plane of the A11 sheet, while $\hat{\boldsymbol{\phi}}_{ROT}$ lies in the local direction of planetary corotation. Adapting the approach of A11, we add an azimuthal field $B_\phi = -\frac{1}{2}\Delta B_\rho$ to represent the azimuthal "bending" of the field lines.

3. Comparison of Plasma Disk Models and T15 Observations

In Figure 2, we show the observed and modeled components of the magnetic field in cylindrical coordinates. The two Ach10 model parameters explored, in order to fit the data, are the effective magnetodisk radius R_{DISK} (which is the equatorial radius of the axisymmetric model's outer boundary/magnetopause) and a proxy for the ring current activity which makes use of the global hot plasma pressure, based on multiorbit statistics of the pressure moments from the Cassini Magnetospheric Imaging Instrument (MIMI) [see *Achilleos et al.*, 2010b; *Sergis et al.*, 2007]. The model field shown is for $R_{DISK} = 40\,R_S$ and average ring current (equivalent to hot plasma pressure $P_H = 2\times10^{-3}$ nPa at Titan's orbit). We show several magnetospheric oscillations. The fits to the amplitude and phase of the B_ρ (radial) and B_ϕ (azimuthal) fields are reasonable, although (i) the displayed B_ρ data show a change in sign during most oscillations, indicative of passage north of the current sheet plane, which is not reproduced with the model, and (ii) the B_ϕ fluctuations show a much steeper "rising" part compared to the model, suggesting that the plasma sheet ripple exhibits structure more complex than a sinusoidal form (equation (1)). The model B_Z is almost in antiphase with the observation, also suggesting additional plasma sheet structure beyond our "wavy disk" model (e.g., a rotating azimuthal anomaly in hot pressure has been proposed by *Brandt et al.* [2010]). Importantly, the predicted fields for a Titan-center-based observer can have significantly different amplitudes and mean values from the fields at the spacecraft, highlighting the need for reliable models in order to predict near-Titan conditions when using data acquired at further distances (>> 50 Titan radii). We show a similar plot in the supporting information for a disturbed ring current model, for which the profile of $P_h\,V_\alpha$, the product of hot plasma pressure and flux tube volume, was increased to twice the values for the "disturbed ring current" of *Achilleos et al.* [2010b], and the disk radius reduced to 35 R_S in order to facilitate obtaining a force balance solution (more details in the supporting information). This disturbed-ring-current model gives better agreement with the amplitudes of the oscillations in B_ρ at times following the Titan encounter.

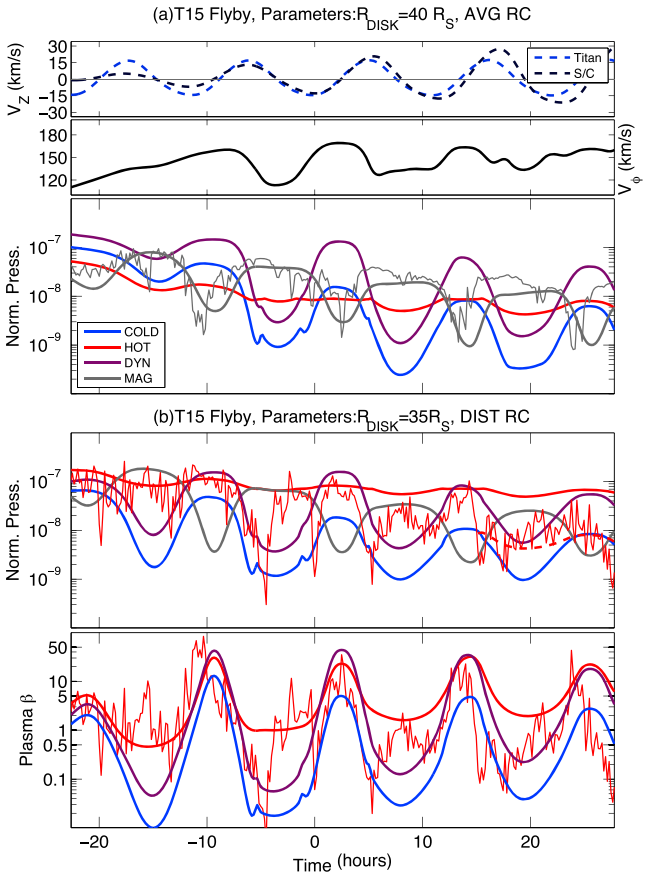

Figure 3. (a) Model predictions for a disk of effective radius $R_{DISK} = 40\ R_S$ and average ring current level (see text). (top) Predicted vertical velocity components for the plasma sheet for the same time interval as Figure 2. (middle) Model azimuthal velocities for the cold plasma on planetary flux tubes conjugate to the spacecraft. (bottom) Predicted pressure contributions, color coded according to physical origin. Pressure is normalized through division by B_o^2/μ_o, where $B_o = 21{,}160$ nT is approximate equatorial field strength at the surface of Saturn. (b) Model predictions for a disk of effective radius $R_{DISK} = 35\ R_S$ and a disturbed ring current level (see text) (using same time interval as Figure 3a). (top) Pressure contributions, color coded according to physical origin (for clarity, the hot pressure model from Figure 3a, at times > 15 h, is shown as a red dashed curve). (bottom) Plasma beta parameters corresponding to the model pressures and to the observed hot plasma/magnetic pressure.

In Figure 3a, we show model plasma parameters corresponding to the field model of Figure 2. The vertical velocity V_Z of the plasma sheet is similar for Titan and Cassini reference frames near closest approach, with values up to ~30 km s^{-1}. Similar vertical velocities were measured by the Cassini plasma spectrometer (CAPS) during the T15 flyby [*Sillanpää et al.*, 2011]. The azimuthal velocity of the cold plasma, lying on field lines conjugate with the spacecraft, is shown in Figure 3a (middle). The largest northward excursions of the plasma sheet (zero-crossing points which occur after the positive maxima in V_Z) are accompanied by decreases in V_ϕ as the spacecraft moves away from the current sheet and connects to flux tubes extending to larger radial distances, which rotate more slowly. Note that V_ϕ for the interval shown, combined with the V_Z for the Titan frame, indicate that the upstream plasma flow direction is tilted with respect to the rotational equator by angles $\lesssim 12°$. The location of maximum magnetic pressure along draped flux tubes would also be expected to deviate from the rotational equator, for appropriate oscillation phases.

The observed magnetic field is dominantly radial outside the current sheet. The maximum value of $|B_\rho/B_Z|$ for the interval shown is ~20, which also equals the maximum ratio $|E_Z/E_\rho|$ for the convective electric field (see *Arridge et al.* [2011a] for more details).

In Figure 3a (bottom), we show the contributions to plasma pressure from various sources. The maximum pressure during current sheet encounters is provided by the dynamic pressure of the cold, subcorotating plasma (violet curve). In the exterior regions or "lobes" of the sheet, magnetic pressure shows local maxima and is the dominant pressure source for this average-ring-current model. The amplitudes and phasing of the observed fluctuations in magnetic pressure (thin gray curve) are in reasonable agreement with the model—although the narrower observed minima suggest a thinner sheet. The hot plasma pressure (red curve) shows relatively weak fluctuations compared to the other curves, since we assume that the hot population has uniform pressure all the way along the field lines. The blue curve indicates thermal pressure of the cold plasma. The total effective pressure predicted by the model near Titan (i.e., dynamic plus thermal plus magnetic) typically increases by a factor of approximately 3 as the current sheet center is approached. This change is mainly due to the variability in dynamic pressure between the sheet center and lobes (the relative change in pressure becomes ~25% if dynamic pressure is excluded). For more information on pressure moments and force balance, see the supporting information.

In Figure 3b, we compare observed and modeled hot plasma pressure using the disturbed-ring-current model described above. Comparing the red curves (Figure 3b, top), the observed hot plasma pressure reasonably agrees with the model over the time interval containing the first three sheet encounters ($\lesssim$ 7 h). Interestingly, the average-ring-current hot pressure model (superposed red dashed curve) is clearly a better match to the data for times later than ~15 h after Titan closest approach. The data show additional variability in hot pressure, partly due to plasma injections and ion beams, which are not explicitly modeled. This disturbed-ring-current model, in comparison to the average-ring-current case (Figure 3a), shows more comparable values of magnetic and hot pressure in the lobes of the sheet (more details of models in the supporting information).

Figure 3b (bottom) shows model plasma beta parameters and the observed hot plasma beta from the Cassini data. The model hot plasma beta (β_h) varies between ~ 0.5 and 30, while the observed β_h reaches values as low as ~ 0.005. A "pseudo" plasma beta may be defined for the dynamic pressure (Ach10) according to $\beta_d = P_{\mathrm{dyn}}/P_{\mathrm{mag}}$, where subscripts indicate dynamic and magnetic pressures. β_d shows local maximum values similar to those for β_h. The thermal cold plasma beta, β_c, shows the lowest model values, down to ~ 2% of β_h. The ratio β_c/β_d has minimum values of ~10%, indicating that the bulk kinetic energy of the cold plasma ions far exceeds their thermal energy.

4. Conclusions

We have calculated a plasma disk model for conditions at the orbit of Titan during the T15 encounter by Cassini. Our model reproduces some of the large-scale variability in the observed magnetic field, although more complex structure for the ripple in the current sheet is required for better agreement. The model outputs are in reasonable agreement with the Cassini observations of magnetic pressure and hot plasma pressure.

For magnetospheric oscillation phases where Titan is farthest from the current sheet, the field is strongly radial and the dominant source of pressure is the magnetic or hot plasma pressure. For phases where Titan is near the center of the sheet, the dominant sources are dynamic and hot plasma pressure. Magnetospheric oscillations also control changes in vertical and azimuthal velocities of the cold plasma for a Titan-based observer. In our model, the incident direction of cold plasma flow may be displaced from Titan's orbital plane by angles of the order ~10°. This result is in good agreement with observations of the plasma flow velocity by *Sillanpää et al.* [2011].

Finally, the plasma disk oscillations and global changes in the hot plasma pressure lead to a wide range of plasma beta regimes in which Titan may be immersed. The hot plasma beta may be as high as ~30 for phases when Titan is at the center of the disk. The cold plasma beta is lower by a factor of ~5 for the model sheet encounter closest to Titan. A pseudo plasma beta associated with the cold plasma dynamic pressure is comparable to or higher than the hot plasma beta near the disk center, depending on ring current state.

This variability in plasma conditions presents a complex requirement for modeling studies. Other models use time-dependent MHD approaches to simulate the plasma flow and periodicities [e.g., *Winglee et al.*, 2013; *Jia et al.*, 2012]. Our model, however, has allowed us to quantify the importance of both hot and cold particle pressure in shaping the near-Titan magnetic and plasma conditions. Our future work will comprehensively explore the response of all near-Titan pressure components and magnetic field to (i) changes in solar wind dynamic pressure and (ii) changes in global hot plasma content. Our model may be used to predict near-Titan conditions from far-field in situ measurements and also to predict plasma moments for observational situations where these are scarce, but magnetic measurements are available.

Acknowledgments
We acknowledge the continued collaboration of the Cassini magnetometer (MAG) and plasma (CAPS and MIMI) instrument teams. N.A. acknowledges useful discussions with colleagues at JAXA and was supported for this work by UK STFC Consolidated grant ST/J001511/1 (UCL Astrophysics). C.S.A. was funded by a Royal Society Research Fellowship. C.B. acknowledges the financial support of the Europlanet Expert Exchange programme. Further details of magnetodisk model outputs and observational data used in this study are available from the first author upon request. N.R. is supported by a PhD grant from CONICET.

The Editor thanks two anonymous reviewers for their assistance in evaluating this paper.

References

Achilleos, N., P. Guio, and C. S. Arridge (2010a), A model of force balance in Saturn's magnetodisc, *Mon. Not. R. Astron. Soc.*, *401*, 2349–2371, doi:10.1111/j.1365-2966.2009.15865.x.

Achilleos, N., P. Guio, C. S. Arridge, N. Sergis, R. J. Wilson, M. F. Thomsen, and A. J. Coates (2010b), Influence of hot plasma pressure on the global structure of Saturn's magnetodisk, *Geophys. Res. Lett.*, *37*, L20201, doi:10.1029/2010GL045159.

Andrews, D. J., A. J. Coates, S. W. H. Cowley, M. K. Dougherty, L. Lamy, G. Provan, and P. Zarka (2010), Magnetospheric period oscillations at Saturn: Comparison of equatorial and high-latitude magnetic field periods with north and south Saturn kilometric radiation periods, *J. Geophys. Res.*, *115*, A12252, doi:10.1029/2010JA015666.

Arridge, C. S., N. Achilleos, and P. Guio (2011a), Electric field variability and classifications of Titan's magnetoplasma environment, *Ann. Geophys.*, *29*, 1253–1258, doi:10.5194/angeo-29-1253-2011.

Arridge, C. S., et al. (2011b), Periodic motion of Saturn's nightside plasma sheet, *J. Geophys. Res.*, *116*, A11205, doi:10.1029/2011JA016827.

Bertucci, C., B. Sinclair, N. Achilleos, P. Hunt, M. K. Dougherty, and C. S. Arridge (2009), The variability of Titan's magnetic environment, *Planet. Space Sci.*, *57*, 1813–1820, doi:10.1016/j.pss.2009.02.009.

Brandt, P. C., K. K. Khurana, D. G. Mitchell, N. Sergis, K. Dialynas, J. F. Carbary, E. C. Roelof, C. P. Paranicas, S. M. Krimigis, and B. H. Mauk (2010), Saturn's periodic magnetic field perturbations caused by a rotating partial ring current, *Geophys. Res. Lett.*, *37*, L22103, doi:10.1029/2010GL045285.

Jia, X., K. C. Hansen, T. I. Gombosi, M. G. Kivelson, G. Tóth, D. L. DeZeeuw, and A. J. Ridley (2012), Magnetospheric configuration and dynamics of Saturn's magnetosphere: A global MHD simulation, *J. Geophys. Res.*, *117*, A05225, doi:10.1029/2012JA017575.

Kurth, W. S., T. F. Averkamp, D. A. Gurnett, J. B. Groene, and A. Lecacheux (2008), An update to a Saturnian longitude system based on kilometric radio emissions, *J. Geophys. Res.*, *113*, A05222, doi:10.1029/2007JA012861.

Lamy, L. (2011), Variability of southern and northern periodicities of Saturn Kilometric Radiation, paper presented at Seventh International Workshop Planetary, Solar and Heliospheric Radio Emissions (PRE VII), Graz, Austria, 15–17 Sept.

Rymer, A. M., H. T. Smith, A. Wellbrock, A. J. Coates, and D. T. Young (2009), Discrete classification and electron energy spectra of Titan's varied magnetospheric environment, *Geophys. Res. Lett.*, *36*, L15109, doi:10.1029/2009GL039427.

Sergis, N., S. M. Krimigis, D. G. Mitchell, D. C. Hamilton, N. Krupp, B. M. Mauk, E. C. Roelof, and M. Dougherty (2007), Ring current at Saturn: Energetic particle pressure in Saturn's equatorial magnetosphere measured with Cassini/MIMI, *Geophys. Res. Lett.*, *34*, L09102, doi:10.1029/2006GL029223.

Sergis, N., S. M. Krimigis, D. G. Mitchell, D. C. Hamilton, N. Krupp, B. H. Mauk, E. C. Roelof, and M. K. Dougherty (2009), Energetic particle pressure in Saturn's magnetosphere measured with the Magnetospheric Imaging Instrument on Cassini, *J. Geophys. Res.*, *114*, A02214, doi:10.1029/2008JA013774.

Sillanpää, I., D. T. Young, F. Crary, M. Thomsen, D. Reisenfeld, J.-E. Wahlund, C. Bertucci, E. Kallio, R. Jarvinen, and P. Janhunen (2011), Cassini Plasma Spectrometer and hybrid model study on Titan's interaction: Effect of oxygen ions, *J. Geophys. Res.*, *116*, A07223, doi:10.1029/2011JA016443.

Simon, S., A. Wennmacher, F. M. Neubauer, C. L. Bertucci, H. Kriegel, J. Saur, C. T. Russell, and M. K. Dougherty (2010), Titan's highly dynamic magnetic environment: A systematic survey of Cassini magnetometer observations from flybys TA-T62, *Planet. Space Sci.*, *58*, 1230–1251, doi:10.1016/j.pss.2010.04.021.

Winglee, R. M., A. Kidder, E. Harnett, N. Ifland, C. Paty, and D. Snowden (2013), Generation of periodic signatures at Saturn through Titan's interaction with the centrifugal interchange instability, *J. Geophys. Res. Space Physics*, *118*, 4253–4269, doi:10.1002/jgra.50397.